

ICEM12- 12th International Conference on Experimental Mechanics
29 August - 2 September, 2004 Politecnico di Bari, Italy

RESIDUAL STRESS MEASUREMENT USING INDENTATION AND A RADIAL ESPI INTERFEROMETER – RECENT PROGRESS

Ricardo Suterio ^(a); Armando Albertazzi Jr. ^(b); Felipe Kleber Amaral ^(b)

^(a) LIT - Test and Integration Laboratory, INPE - National Institute for Space Research, São José dos Campos - SP - Brazil, suterio@lit.inpe.br

^(b) Labmetro - Automation and Metrology Laboratory, UFSC - Federal University of Santa Catarina, 88040-970 - Florianópolis - SC - Brazil, albertazzi@labmetro.ufsc.br

ABSTRACT

*A new kind of electronic speckle pattern interferometer (ESPI) was developed by the authors' group using conical mirrors to measure the radial in-plane displacement component. True radial in-plane sensitivity is achieved by double illumination. This device is used in this paper to measure residual stresses in combination with the indentation method. A semi-empirical mathematical model is developed to quantify the residual stresses. Several tests were made in a specimen with different levels of residual stresses imposed by a mechanical loading. Empirical constants were computed from those tests and are used in combination with the developed model to predict the residual stresses levels. The tests presented here are preliminary since they are restricted to only one material, one-axis stress state, one geometry of the indentation tip and only one indentation force. In these conditions the results are very encouraging since a typical measurement error of about 5% was found for the principal residual stress. **Keywords:** residual stress, indentation, ESPI; radial interferometer.*

1. INTRODUCTION

In many applications, it is very important to know the magnitude and direction of residual stresses. Since residual stresses are very difficult to be predicted using analytical or numerical models, their values are very often determined by direct measurement by experimental methods. One of the most widely used experimental methods is the hole-drilling technique. This technique involves monitoring the strains produced when a small hole is drilled into a stressed material. The drilled hole produces a local release of residual stresses that are measured by a special type of strain gauges. Those values are used into an appropriate mathematical method to quantify the residual stresses level^[4].

Alternatively, it is possible to obtain qualitative information about the residual stresses acting in a material by the indentation method^{[7],[8]}. The main idea is to produce a local indentation print using a tool with a conical or spherical tip and a controlled level of loading or total energy. In opposition to the hole drilling method, the indentation does not release stresses but add more stresses creating a local plastic zone. The local plastic deformation is a function of the geometry of the indentation tip, material properties, and is also strongly dependent of the magnitude and direction of the residual stresses initially present in the material. Previous works had reported different attempts to quantify residual stresses using the indentation method from: (a) hardness variation measurement; (b) relation between force and indentation depth; (c) the final geometric shape of the indentation print and (d) deformation or displacement measured around the indentation print^{[2],[3],[7],[8]}. This behavior is

very difficult to be analytically and numerically modeled and it is not usually used for quantitative measurement in a very accurate way.

Preliminary results of a quantitative evaluation of residual stresses measurement using indentation is reported in this paper. An indentation print is produced in the region where residual stresses have to be measured. The in-plane radial displacement is measured around it. There is a clear correlation between the residual stresses level and the fringe pattern developed around the indentation print. A semi-empirical mathematical model was developed using the hole drilling model as a starting point. Additional parameters were added to this model to best represent the actual measured data. The possibilities to use those additional parameters to quantify the residual stresses are here investigated.

2. THE RADIAL INTERFEROMETER

A double illumination radial in-plane interferometer (RIP) using ESPI is used in this paper^[1]. The basic principle is shown in figure 2.1. This interferometer was recently incorporated in a portable and modular device for residual stresses measurement.

The main optical element of the interferometer is a conical mirror, which is placed near the specimen surface. Figure 2.1(a) shows a cross-section of the conical mirror containing the mirror axis, which displays two particularly chosen light rays from a collimated illumination source. Each light ray is reflected by the conical mirror surface towards a point P over the specimen surface, reaching this point symmetrically. The illumination directions are indicated by the unitary vectors \mathbf{n}_A and \mathbf{n}_B and they have the same angle with respect to the surface normal. The sensitivity direction is given by the vector \mathbf{k} obtained from the subtraction of the two unitary vectors. Therefore, in-plane sensitivity is reached in point P as well as in any other point on the circular double illuminated area. The only exception is the central point, there is a singular point.

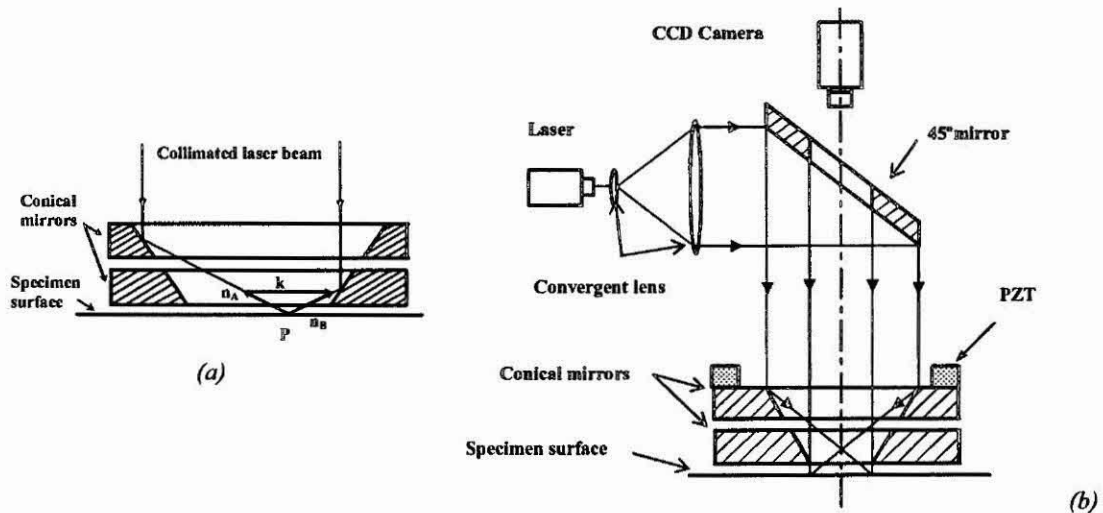


Figure 2.1 Double illumination through the radial interferometer.

A practical configuration of the radial in-plane interferometer is shown in figure 2.1(b). The laser light is expanded and collimated. The collimated beam is reflected towards the conical mirror using a 45° tilted mirror. The central circular window located at this mirror has two main functions: (a) to avoid that the laser light to reach directly the measured surface to prevent triple illumination, and (b) to provide a viewing window for the camera. The conical mirror is formed by two parts with a small gap between them that is controlled by a PZT actuator do produce phase shifting.

3. RESIDUAL STRESS MEASUREMENT

In order to measure residual stresses usually a small hole is drilled in the center of the measured area. A mathematical developed by Kirsch^[4] based on the elastic solution for an infinite plate, subjected to a uniform state of stresses, with a cylindrical hole drilled all way through the plate thickness, is used. According to that, the radial component of the displacement field (u_r), developed by the hole drilling in polar coordinates is^{[11],[5]}:

$$u_r(\rho, \theta) = A(\rho)(\sigma_1 + \sigma_2) + B(\rho)(\sigma_1 - \sigma_2) \cos(2\theta - 2\beta) \quad (3.1)$$

where the functions $A(\rho)$ and $B(\rho)$ are given by:

$$A(\rho) = \frac{(1+\nu)}{2E} r_0 \rho \quad B(\rho) = \frac{1}{2E} r_0 [4\rho - (1+\nu)\rho^3] \quad (3.2)$$

and, r, θ are polar coordinates;
 r_0 is the drilled hole radius;
 ρ is the normalized radius ($\rho = r_0 / r$);
 σ_1, σ_2 are the principal residual stresses (maximum and minimum respectively);
 E is the material's Young modulus;
 ν is the material's Poisson ratio;
 β is the principal direction.

Figure 3.1(a) shows a typical radial displacement phase difference pattern for a one-axis residual stress state due to hole drilling method combined with ESPI. The hole of diameter is 0.8 mm and the residual stress is about 200 MPa.

In opposition to the hole drilling method, the indentation print does not release the stresses, but add more stresses, producing a local yielding. As a consequence, a permanent displacement field is produced around it. In a stress-free material, this permanent displacement field is axi-symmetrical and repeatable if the indentation tip geometry, indentation loading and material properties are constant. If mechanical or residual stresses are present in the material prior the indentation, the permanent displacement field is affected in a way that depends on the residual stresses levels.

Figure 3.1(b) to (d) show some experimental results. Those phase difference patterns are related to the radial displacement component, measured by the radial in-plane ESPI interferometer. The indentation was made using a 120° conic tip. Figure 3.1(b) shows the radial displacement in a stress-free material. Figure 3.1(c) shows the radial displacement in a material with a one-axis 200 MPa stresses field aligned about 30° with the horizontal axis, and figure 3.1(d) shows the resulting phase difference between the two previous phase patterns.

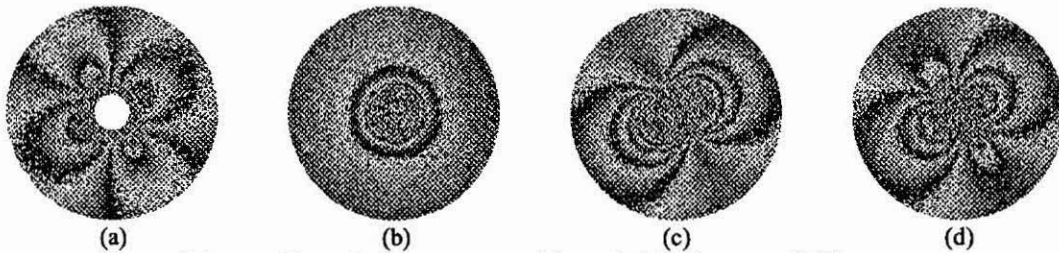


Figure 3.1 Typical phase patterns of the radial displacement fields component:
 (a) for Hole Drilling Method (computer simulated), (b) in a stress-free material after indentation,
 (c) with 200 MPa stress after indentation, and (d) phase difference: (c - b)

Comparing figure 3.1(a) and figure 3.1(d) it is possible to see that, after removing the permanent displacement field related to a stress-free material, there is a strong similarity between them.

In order to find a model to measure residual stresses the authors' approach uses this similarity. A mathematical model was derived starting from equation (3.1). It is noted that the term that depend on $\cos(2\theta)$ is related to the principal stresses difference ($\sigma_1 - \sigma_2$) and the term independent of θ is related to the principal stresses sum ($\sigma_1 + \sigma_2$). The radial component of the displacement field (u_r), is here modeled in polar coordinates by the following equation:

$$u_r(r, \theta) = \frac{K_1}{r} + \left(\frac{K_2}{r} + \frac{K_3}{r^3} \right) \cos(2\theta - 2\beta) \quad (3.3)$$

where K_1 , K_2 and K_3 are unknown functions given by:

$$K_1 = f[(\sigma_1 + \sigma_2), E, \nu], K_2 = g[(\sigma_1 - \sigma_2), E, \nu], \text{ and } K_3 = h[(\sigma_1 - \sigma_2), E, \nu] \quad (3.4)$$

It was experimentally verified that the radial displacement on a stress-free material can be reasonably described using the equation proposed by Giannakopoulos & Suresh - 1997^[2]:

$$u_r(r) = K \frac{\nu}{E(\nu-1)} \frac{1}{r^{\frac{1}{\nu-1}}} \quad (3.5)$$

where K is a constant that depends upon the indentation force, tip geometry and materials properties.

This constant can be determined by fitting this model to experimental data from the radial displacement field measured after indenting a stress-free specimen of the same material in identical conditions. So, the complete model to relate residual stress with the radial displacement field is given by:

$$u_r(r, \theta) = \frac{K_1}{r} + \left(\frac{K_2}{r} + \frac{K_3}{r^3} \right) \cos(2\theta - 2\beta) + K_4 \frac{\nu}{E(\nu-1)} \frac{1}{r^{\frac{1}{\nu-1}}} \quad (3.6)$$

where K_4 is equivalent to constant "K" in equation (3.7), determined a priori in a stress-free specimen.

4. MEASUREMENT SYSTEM AND EXPERIMENTAL SETUP

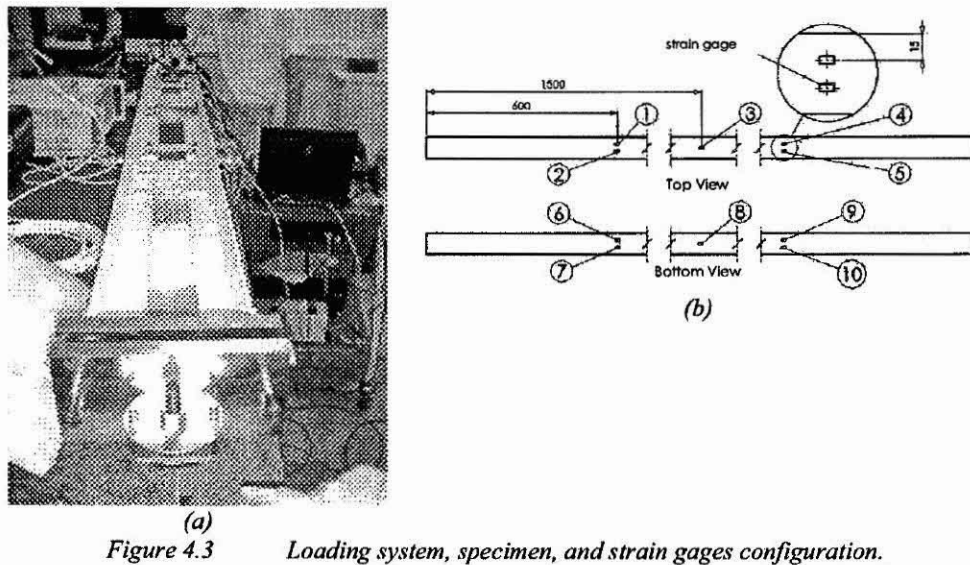
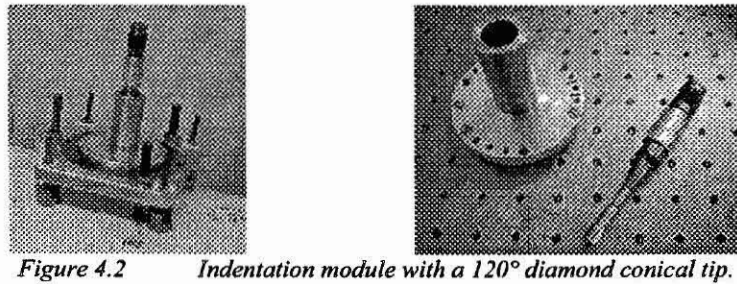
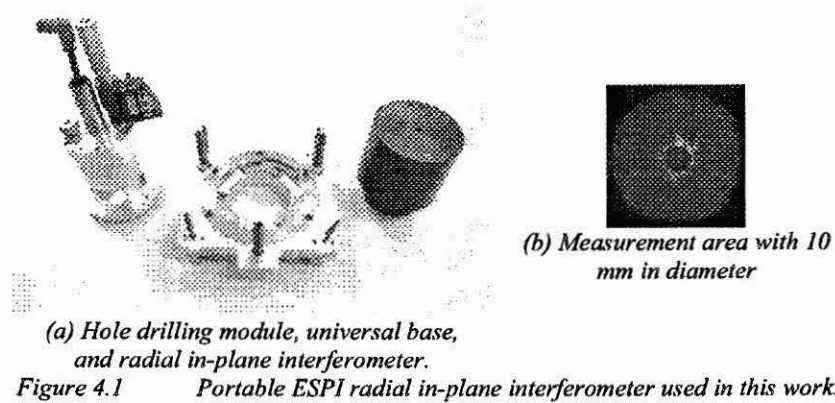
Figure 4.1(a) shows the portable ESPI radial in-plane interferometer used in this paper. The system is composed by a diode laser source with 658 nm wavelength, a 30° conical mirror and a CCD camera. The illuminated region is about 10 mm in diameter (figure 4.1b).

The indentation module used a constant impact energy printed through a conical diamond 120° indenter tip (see figure 4.2).

In order to validate this model, reference values for residual stresses are necessary. It is very difficult or expensive to find a known residual stresses reference standard. In order to overcome this difficulty, known residual stresses fields were mechanically simulated by the device shown in figure 4.3(a). Basically, a long residual-stresses free specimen is loaded by traction through 6 bolts connected to a "U" shaped structure.

The specimen is a rectangular steel bar with approximate dimensions of 3 x 50 x 3000 mm (figure 4.3b). The long specimen was instrumented with ten strain gages to monitoring

the actual tension level applied to the specimen guarantee uniform loading and to provide a reference value for it. The specimen size is long enough to accommodate over 300 measurement points. The portable radial in-plane interferometer was clamped to the loading in such a way that its measurement axis was aligned in about 30° with the loading direction.



5. EXPERIMENTAL RESULTS

A set of measurement tests was planned and executed with eight different stresses levels. In all cases the same long specimen made of AISI 1020 steel was indented with a 120° conic tip, using about the same amount of energy given by a mechanical impact of a sphere driven by a spring at constant compression rate. The sampling region was delimited by two

circles concentric with the indentation print with radius 1.5 and 4.5 mm. A mesh of 12 x 360 = 4320 measurement points was used for the calculations.

Several measurement points were indented in different positions of the same long specimen. The uncertainty of each reference value was found to range from 5 to 9% for 95% confidence level^[6]. Figure 3.1(a) shows the result of indenting a stress-free material. From this data the value of the constant K in equation (3.5) was determined by least squares fitting and its value becomes K_4 in equation (3.6).

Figure 5.1 show results for different stresses levels. In all cases, the left image is the total radial displacement field. The image on right is the difference computed from the total radial displacement (left image) minus the radial displacement field for the stress-free state computed from figure 3.1(a).

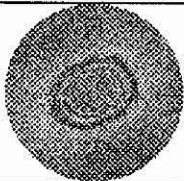
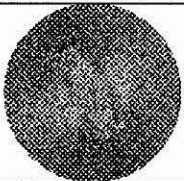
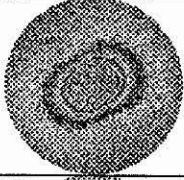
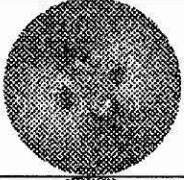
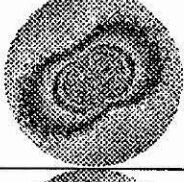
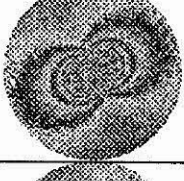
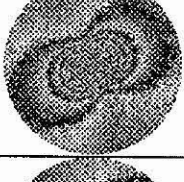
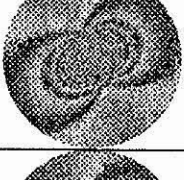
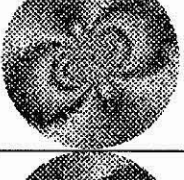
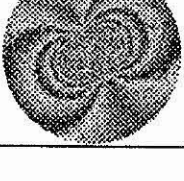
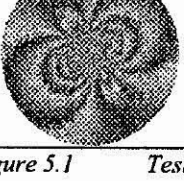
		Test at 59.7 MPa Image: 142.tif Measurement Output $\beta : 27.4^\circ$
		Test at 80.2 MPa Image: 143.tif Measurement Output $\beta : 27.8^\circ$
		Test at 100.1 MPa Image: 135.tif Measurement Output $\beta : 30.4^\circ$
		Test at 120.1 MPa Image: 136.tif Measurement Output $\beta : 26.1^\circ$
		Test at 139.7 MPa Image: 137.tif Measurement Output $\beta : 27.9^\circ$
		Test at 159.9 MPa Image: 138.tif Measurement Output $\beta : 28.0^\circ$
		Test at 199.5 MPa Image: 139.tif Measurement Output $\beta : 29.7^\circ$

Figure 5.1 Test results.

The values for K_1 to K_3 were computed from those images and are presented in table 1. Figure 5.2 plot the relation between those constants and the reference stress level ($\psi_1 \times K_1$, $\psi_2 \times K_2$, and $\psi_3 \times K_3$), where: ψ_1 , ψ_2 and ψ_3 are the reference stress level. In this particular case both sum and difference of principal stresses are equal since $\sigma_2 = 0$.

It is clear a linear behavior between K_1 and the reference stress for levels above 100 MPa as well as for K_2 and the reference stresses for this same level.

The linear relation between K_3 and the reference stress is not clear. Linear regression lines were fitted in order to predict both principal stresses sum and difference from K_1 and K_2 respectively. From those predicted values, σ_1 and σ_2 were computed by: $\sigma_1 = (\psi_1 + \psi_2) / 2$ and $\sigma_2 = (\psi_1 - \psi_2) / 2$. The resulting values are presented in table 2. Note that for stresses levels over 100 MPa the agreement is very good. For values less than 100 MPa apparently the indentation signal is not strong enough.

Table 1 Constants K_1 through K_3 determined using least square fitting

Image	ϵ_{ref} [$\mu\text{m}/\text{m}$]	σ_{ref} [MPa]	K_1	K_2	K_3	K_4
I39.tif	997.5	199.5	0.001096724	0.001049659	0.000623278	
I38.tif	799.5	159.9	0.000897067	0.000788120	0.000434033	
I37.tif	698.5	139.7	0.000715604	0.000657062	0.000379679	
I36.tif	600.5	120.1	0.000551835	0.000619662	0.000365282	-790.6
I35.tif	500.5	100.1	0.000624862	0.000447222	0.000432281	
I43.tif	401.0	80.2	0.000219474	0.000168717	0.000502606	
I42.tif	298.5	59.7	0.000059478	0.000146770	0.000391771	

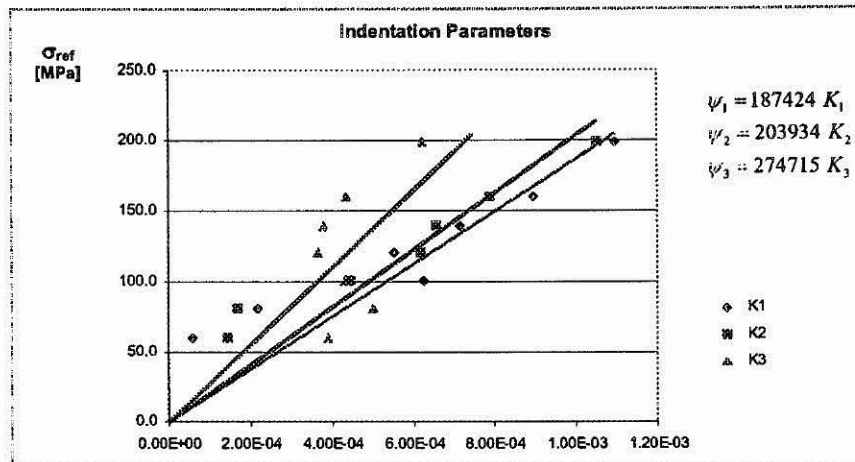


Figure 5.2 Indentation parameter versus reference residual stress.

Table 2 Predict values through the indentation parameter interpolation

Ref. Value [MPa]	Relative to Yield Point	Predict Values		Difference Error	
σ_{ref} [MPa]	σ_{ref} / σ_e	σ_1 [MPa]	σ_2 [MPa]	$\sigma_{ref} - \sigma_1$ [MPa]	$(\sigma_{ref} - \sigma_1) / \sigma_{ref}$
199.5	67.6%	209.8	-4.3	10.3	5%
159.9	54.2%	164.4	3.7	4.5	3%
139.7	47.4%	134.1	0.1	-5.6	-4%
120.1	40.7%	114.9	-11.5	-5.2	-4%
100.1	33.9%	104.2	13.0	4.1	4%
80.2	27.2%	37.8	3.4	-42.4	-53%
59.7	20.3%	20.5	-9.4	-39.2	-66%

6. CONCLUSIONS

This paper investigates the possibility to quantify residual stresses combining the indentation method with a radial in-plane ESPI interferometer. The classical model was modified by introducing three unknown functions. Experimental data from eight stresses states were fitted to this model and the resulting parameters were analyzed. A linear relationship was found between the residual stresses induced level and two parameters and it was used to predict the residual stresses from the measured radial displacement field. Agreement of about 5% was found for five residual stresses levels above 100 MPa. As a preliminary evaluation the results were considered very encouraging. It is clear that K_1 and K_2 in equations (3.3) or (3.8) are good choices to be correlated with the residual stresses sum and differences respectively. The term K_3 has not a clear relationship what points that the mathematical model of equations (3.3) or (3.8) have to be modified replacing the term that depends on r^{-3} to another more convenient function.

However those results are restricted to very specific conditions. Only one material was involved, only one-axis residual stresses induced was analyzed, only one indentation tool with constant energy was used. Further work will be focused on extending those conditions. Initially indentation tools with spherical shape will be investigated as a way to increase measurement sensitivity in lower stresses levels. Next, different materials will be investigated. Finally, different residual stresses states will be investigated.

The final goal of this research work is to develop a portable residual stresses measurement unit. The authors believe that the combination of indentation and this radial in-plane ESPI interferometer can be the basis for a very practical device.

ACKNOWLEDGMENTS

The authors would like to thank the institutions that have been support this work: ANP-PRH34, CTPETRO, PADCT, CNPq/RHAE and CAPES.

REFERENCES

- [1] ALBERTAZZI JR, A.; KANDA, C; BORGES, M. R.; HREBABETZKY, F. - "*Portable Residual Stresses Measurement Device Using ESPI and a Radial In-Plane Interferometer*" - Laser Metrology for Precision Measurement and Inspection in Industry; Albertazzi Jr., A.; Eds., Proc. SPIE, v. 4420, p. 112-122, Sep. 2001.
- [2] GIANNAKOPOULOS, A. E.; SURESH, S. - "*Indentation of Solids with Gradients in Elastic Properties. Part I: Point Force*" - Journal of Solids and Structures, v.34, n.19, p.2357-2392, 1997.
- [3] GIANNAKOPOULOS, A. E.; SURESH, A. - "*Theory of Indentation of Piezoelectric Materials*" - Elsevier Science Ltd., Acta Materialia, v.47 n.7 p.2153-2164, 1997.
- [4] LU, JIAN - "*Handbook on Measurement of Residual Stresses*" - The Fairmont Press, SEM - Society for Experimental Mechanics, GA, USA, 1996.
- [5] MAKINO, A.; NELSON D. - "*Residual-Stress Determination by Single-Axis Holographic Interferometry and Hole Drilling. Part I: theory*" - Exp. Mech. 34, 66-78 (1994).
- [6] SUTERIO, R.; ALBERTAZZI JR., A. G.; PACHECO, A.; FERREIRA, R. P. - "*Metrology Analysis of a Simulation Device for Residual Stress*" (in Portuguese) - METROLOGIA 2003 – Brazilian Congress of Metrology, SBM –Brazilian Society of Metrology, Recife, PB, Brazil, sep. 1-5 , 2003.
- [7] SUTERIO, R; ALBERTAZZI JR., A. G.; CAVACO, M. A. M. - "*Preliminary Evaluation: The Indentation Method Combined with a Radial Interferometer for Residual Stress Measurement*" - SEM Annual Conference and Exposition on Experimental and Applied Mechanics, SEM - Society for Experimental Mechanics, Charlotte, North Carolina, USA, June 2-4, 2003.
- [8] UNDERWOOD, J. H. - "*Residual Stress Measurement using Surface Displacements around an Indentation*" - Experimental Mechanics, p. 373-380, Sep., 1973.